Throughput Behavior in Multi-Hop Multi-Antenna Wireless Networks

Bechir Hamdaoui and Kang G. Shin

***Abstract*— Multi-antenna or MIMO systems offer great potential for increasing the throughput of multi-hop wireless networks via spatial reuse and/or spatial multiplexing. This paper characterizes and analyzes the maximum achievable throughput in multi-hop, MIMO-equipped, wireless networks under three MIMO protocols, *spatial reuse only* (SRP), *spatial multiplexing only* (SMP), and *spatial reuse & multiplexing* (SRMP), each of which enhances the throughput, but via a different way of exploiting MIMO's capabilities. We show via extensive simulation that as the number of antennas increases, the maximum achievable throughput first rises and then flattens out asymptotically under SRP, while it increases "almost" linearly under SMP or SRMP. We also evaluate the effects of several network parameters on this achievable throughput, and show how throughput behaves under these effects.**

***Index Terms*— End-to-end network throughput, MIMO systems, multi-hop wireless networks.**

I. Introduction

Multi-antenna or MIMO (multiple-input multiple-output) systems have great potential for increasing the throughput of multi-hop wireless networks through *spatial spectrum reuse* by allowing multiple simultaneous communications in the same neighborhood and/or through *spatial division multiplexing* by achieving high data rates. Therefore, MIMO systems are considered as a key technological solution to next-generation wireless networking and communication problems, such as the bandwidth-shortage problem [1], [2].

From the physical layer's standpoint, the potential benefits of MIMO are already well-understood and characterized for the single, point-to-point communication link [3], [4], [5], [6], [7]. How to realize these benefits at higher layers has also been studied recently [8], [9], [10], [11], [12], [13]. These studies focused on the development of MAC protocols for wireless networks that exploit MIMO to increase the overall network throughput via spatial reuse [12], [13] and/or spatial multiplexing [9], or reduce power consumption via beam-forming and interference suppression [8]. However, how much throughput MIMO can offer multi-hop wireless networks has been studied much less [14]. Yi *et al.* [14] extended the work in [15] to wireless networks using directional antennas. The focus in [14] is, however, on the switched multi-beam technique. Albeit simple, the switched multi-beam technique works only in a near line-of-sight environment, and may increase the capacity only through spatial reuse. In this paper, we characterize and analyze the maximum achievable throughput in multi-hop wireless MIMO networks when the adaptive array technique is used. Unlike the switched multi-beam technique, the adaptive array technique can exploit multiple antennas to increase the capacity in both line-of-sight and multi-path environments [16] via not only spatial reuse but also spatial multiplexing.

In this paper, we make the following contributions.

1) Design and modeling of interference and radio constraints on multi-hop wireless MIMO networks under three MIMO protocols and two interference avoidance models that we propose.
2) Characterization and analysis of the maximum achievable throughput in multi-hop wireless MIMO networks. Via extensive simulations, we show that as the number of antennas increases, the maximum achievable throughput flattens out asymptotically under SRP and increases "almost" linearly under SMP or SRMP.
3) Evaluation of the effects of several network parameters on the achievable network throughput. We show how the network throughput performance behaves under the effects of such parameters.

The rest of this paper is organized as follows. Section VIII discusses the related work, putting our work in a comparative perspective. Section II overviews MIMO and illustrates its potential benefits. We model the network under study and state our objectives in Section III. Section V models the packet-level constraints, while Section VI formulates the multi-commodity flow routing problem. Throughput characterization and analysis are provided in Section VII. Finally, we conclude the paper in Section IX.

II. MIMO Links

A. Basics of MIMO

Let us consider the MIMO link shown in Fig. 1(a), and assume that the transmitter and the receiver are each equipped with 2 antennas. To transmit a signal $s(t)$ over the 2-antenna array, the transmitter sends two weighted copies, $u_1 s(t)$ and $u_2 s(t)$, of the signal, one on each antenna; the vector[1] $\mathbf{u} = [u_1 \ u_2]^T$ is referred to as a *transmission weight vector*. At the receiver, the two received signals (one on each antenna) are weighted with a *reception weight vector* $\mathbf{v} = [v_1 \ v_2]^T$ and summed to produce $r(t)$. This is illustrated in Fig. 1(b). Let $\mathbf{H}$ denote the matrix of channel coefficients between the transmitter and the receiver. One can then write $r(t) = (\mathbf{u}^T \mathbf{H} \mathbf{v}) s(t)$. By choosing appropriate weight vectors $\mathbf{u}$ and $\mathbf{v}$, one can ensure that the signal $r(t)$ achieves a unit gain ($\mathbf{u}^T \mathbf{H} \mathbf{v} = 1$) when received by the target receiver, and a zero gain ($\mathbf{u}^T \mathbf{H} \mathbf{v} = 0$) when received by a non-target receiver. Hence, with multiple antennas, a node

This work was supported by NSF under Grant CNS-0721529.

Bechir Hamdaoui is with the School of EECS at Oregon State University. Kang G. Shin is with the Department of EECS at the University of Michigan. Emails: hamdaoui@eecs.orst.edu; kgshin@eecs.umich.edu.

[1]The superscript ^{T} indicates the matrix transpose operation.

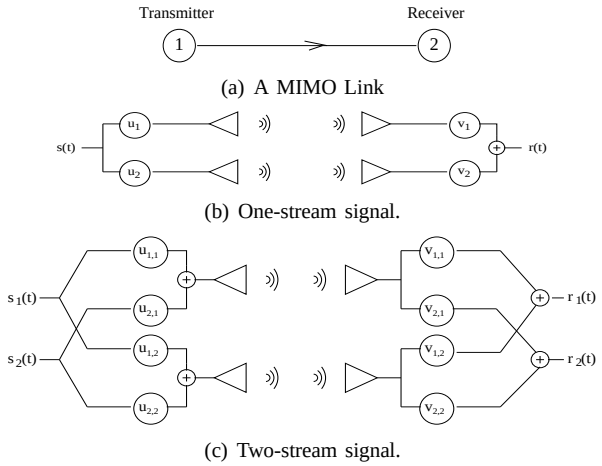

(a) A MIMO Link

(b) One-stream signal.

(c) Two-stream signal.

Fig. 1. MIMO processing.

can successfully communicate with its target receiver while allowing other nearby receivers to successfully receive their signals.

Multiple antennas can also be exploited to send multiple-stream signals. As shown in Fig. 1(c), the transmitter can send two streams, $s_1(t)$ and $s_2(t)$, each weighted over both antennas using the transmission weight vectors $\mathbf{u}_1 = [u_{1,1}\ u_{1,2}]^T$ and $\mathbf{u}_2 = [u_{2,1}\ u_{2,2}]^T$, respectively. At the receiver, two separate streams, $r_1(t)$ and $r_2(t)$, are constructed by weighting the two received signals (one on each antenna) by two reception weight vectors $\mathbf{v}_1 = [v_{1,1}\ v_{1,2}]^T$ and $\mathbf{v}_2 = [v_{2,1}\ v_{2,2}]^T$. One can write $r_1(t) = (\mathbf{u}_1^T\mathbf{H}\mathbf{v}_1)s_1(t) + (\mathbf{u}_2^T\mathbf{H}\mathbf{v}_1)s_2(t)$ and $r_2(t) = (\mathbf{u}_1^T\mathbf{H}\mathbf{v}_2)s_1(t)+(\mathbf{u}_2^T\mathbf{H}\mathbf{v}_2)s_2(t)$. With an appropriate choice of all the weight vectors and under the assumption that $\mathbf{H}$ is a full-ranked matrix [7], one can ensure that $\mathbf{u}_1^T\mathbf{H}\mathbf{v}_1 = 1$ and $\mathbf{u}_2^T\mathbf{H}\mathbf{v}_1 = 0$ to correctly construct $r_1(t)$, and $\mathbf{u}_1^T\mathbf{H}\mathbf{v}_2 = 0$ and $\mathbf{u}_2^T\mathbf{H}\mathbf{v}_2 = 1$ to correctly construct $r_2(t)$. Hence, multiple antennas can be exploited to *increase* the data rates by sending multiple-stream signals.

We will henceforth use $\mathbf{u}_{m,i}$ to denote node m's $\gamma_m \times 1$ weight vector used to transmit its i^{th} stream of data, where γ_m is the number of elements of m's antenna array. Node m uses the j^{th} element ($u_{m,i,j}$) of this vector to weigh the i^{th} transmitted stream on the j^{th} element of the antenna array. If only one stream of data is being transmitted by m, the notation $\mathbf{u}_m$ will be used to denote the transmission weight vector. Also, $\mathbf{v}_{m,i}$ will be used to denote node m's $\gamma_m \times 1$ reception weight vector used to receive its i^{th} stream of data. The j^{th} element ($v_{m,i,j}$) of this vector is used by m to weigh the i^{th} received stream on the j^{th} element of the antenna array. If only one stream is being received by m, the notation $\mathbf{v}_m$ will then be used instead.

B. Benefits of MIMO

To illustrate MIMO benefits, let's consider the example of a multi-hop wireless MIMO network in Fig. 2, which consists of a set $N = \{1, 2, 3, 4\}$ of 4 nodes, and a set $L = \{(1, 3), (2, 4), (1, 4)\}$ of MIMO links. Suppose each node has 2 antennas ($\gamma_m = 2, \forall m \in N$).

Fig. 2. An illustrative network example.

1) Spatial Reuse: Due to multiple antennas, transmitters can null their signals at undesired nearby receivers (i.e., prevent their signals from reaching undesired nearby receivers) while ensuring acceptable signal gains at their desired receivers. Likewise, receivers can use their multiple antennas to suppress interferences caused by undesired nearby transmitters while successfully receiving their desired signals. For the purpose of illustration, let's assume that, at a given time t, nodes 1 and 2 both decided to transmit signals to nodes 3 and 4, respectively. First, note that if nodes are equipped with single omnidirectional antennas, then node 1's transmission will interfere with node 4's reception, and hence, node 4 won't be able to successfully receive the signal from node 2. Because node 4 has 2 antennas, its reception weight vector $\mathbf{v}_4$ can be so chosen that the interference caused by node 1's transmission may be suppressed while assuring an acceptable gain of its intended signal from node 2. These constraints or requirements can be written as $(\mathbf{u}_2^T\mathbf{H}_{2,4})\mathbf{v}_4 = 1$ and $(\mathbf{u}_1^T\mathbf{H}_{1,4})\mathbf{v}_4 = 0$ where $\mathbf{u}_2 = [u_{2,1}\ u_{2,2}]^T$ is the transmission weight vector of node 2 and $\mathbf{v}_4 = [v_{4,1}\ v_{4,2}]^T$ is the reception weight vector of node 4. Knowing $\mathbf{H}_{1,4}$, $\mathbf{H}_{2,4}$, $\mathbf{u}_1$, and $\mathbf{u}_2$, node 4 can solve the system of these two equations to determine $\mathbf{v}_4^*$ which can then be used to receive an interference-free signal from node 2 *concurrently* with node 1's transmission signal. Multiple antennas can thus be exploited to increase *spatial reuse* by allowing multiple simultaneous transmissions in the same vicinity.

2) Spatial Division Multiplexing: Suppose node 1 does not transmit at time t, then node 4 can use both antennas to receive two streams of data concurrently. To design its reception weight vectors $\mathbf{v}_{4,1} = [v_{4,1,1}\ v_{4,1,2}]^T$ and $\mathbf{v}_{4,2} = [v_{4,2,1}\ v_{4,2,2}]^T$, we need to solve two systems of linear equations

$$\begin{cases} (\mathbf{u}_{2,1}^T\mathbf{H}_{2,4})\mathbf{v}_{4,1} = 1 \\ (\mathbf{u}_{2,2}^T\mathbf{H}_{2,4})\mathbf{v}_{4,1} = 0 \end{cases} \quad \text{and} \quad \begin{cases} (\mathbf{u}_{2,1}^T\mathbf{H}_{2,4})\mathbf{v}_{4,2} = 0 \\ (\mathbf{u}_{2,2}^T\mathbf{H}_{2,4})\mathbf{v}_{4,2} = 1 \end{cases}$$

where $\mathbf{u}_{2,1} = [u_{2,1,1}\ u_{2,1,2}]^T$ and $\mathbf{u}_{2,2} = [u_{2,2,1}\ u_{2,2,2}]^T$ are the two transmission weight vectors used by node 2 to transmit its two streams. The solution can then be used by node 4 to receive two concurrent data streams from node 2. Hence, multiple antennas can also be used to increase the transmission rates by exploiting the *spatial multiplexing* offered by the antennas. Note that now, node 1 cannot transmit without causing interference at node 4; spatial reuse cannot be increased when multiple antennas are used for spatial multiplexing.

C. Practical Considerations

Although this paper focuses on the characterization of the maximum achievable throughput, and hence, it ignores irrelevant aspects, such as how and when nodes exchange channel coefficients, it is worth reviewing some of them for completeness. Channel estimation is one practical aspect that is crucial to enable MIMO capabilities. Nodes should be

able to estimate channel coefficients in order to solve the optimization formulations illustrated earlier. Many channel estimation techniques [17], [18], [19], [20] have already been proposed in literature, which can be categorized into two types: pilot-assisted techniques (e.g., [17], [20]) and blind techniques (e.g., [18], [19]). For pilot-assisted techniques, channel coefficients can be estimated by exploiting the frequency and/or the time correlation of the pilot and data symbols. Blind estimation techniques, on the other hand, exploit the statistical properties or the deterministic information of the transmitted symbol. Nodes can then use any of these proposed techniques to estimate their channel coefficients.

In general, maintaining up-to-date knowledge of these coefficients on a per-packet basis may be very challenging due to time-varying channel conditions. In this paper, however, channel conditions need to remain constant only during a single communication so that nodes can update their channel coefficients at the beginning of every communication, and assume them to stay unchanged until the communication is completed. In certain wireless settings and applications, such as sensor and mesh networks, channel coefficients usually experience little variability since these networks are static (nodes do not move) and are deployed in un-noisy (non-urban) areas.

Nodes also need to exchange channel information as well as antenna weight vectors among themselves. Protocols, such as NULLHOC [21] and others, have already been proposed to enable information exchange among nodes for sharing the wireless medium. Once it acquires knowledge of channel information, each node can use a centralized or a distributed approach to select its transmission and reception weight vectors. The centralized approach requires global knowledge of information, i.e., a global center gathers all necessary information and solves an optimization problem to find all weight vectors. This approach, albeit impractical, provides the optimal solution in terms of overall network throughput. The distributed approach, which we adopt in this paper as illustrated in Section II-D, requires that each new transmitter be responsible for avoiding interference with existing flows by adjusting its transmission weight vectors. That is, a new transmitter first gathers weight vectors from its neighbors, and then uses them to determine its transmission vector. This, however, requires some form of collaboration between the new transmitter and its immediate neighbors.

D. Interference Models: Cooperative vs. Non-cooperative

We now propose two models[2] that can be used by nodes to suppress interference and/or null undesired signals so that the spatial reuse of spectrum may be increased.

Non-Cooperative Interference Avoidance Model (NiM): This model requires that (1) transmitters be responsible for nulling their signals at all nearby interfering receivers prior to transmitting their signals, and (2) receivers be responsible for suppressing the interference caused by all nearby transmitters prior to receiving their desired signals. That is, before transmitting its signal, a transmitter must ensure that it has enough antennas to transmit the signal without causing interference to any of its nearby receivers. Likewise, prior to receiving signals, a receiver must ensure that it has enough antennas to be able to suppress the interference caused by all nearby transmitters while receiving its desired signals without interference. In the example network of Fig. 2, under NiM, node 4 must then be able to suppress node 1's signal prior to receiving node 2's signal, and node 1 must be able to null its signal at node 4 prior to transmitting a signal to node 3.

Cooperative Interference Avoidance Model (CiM): Note that it suffices for node 4 to suppress node 1's signal, or for node 1 to null its signal at node 4 to have two successful transmissions. Unlike NiM, CiM requires that either the transmitter or the receiver (not necessarily both) be responsible for interference avoidance. Referring to the example of Fig. 2 again, nodes 1 and 4 must then coordinate to design their vectors such that

$$\begin{cases} \mathbf{u}_1^T(\mathbf{H}_{1,3}\mathbf{v}_3) = 1 & \text{(ensured by node 1)} \\ \mathbf{u}_1^T\mathbf{H}_{1,4}\mathbf{v}_4 = 0 & \text{(ensured by either node 1 or node 4)} \\ (\mathbf{u}_2^T\mathbf{H}_{2,4})\mathbf{v}_4 = 1 & \text{(ensured by node 4).} \end{cases}$$

Clearly, CiM provides higher spatial reuse of multiple antennas than NiM. This will be justified later.

E. Interference Models: Limitations and Implications

Deriving interference models for multi-hop settings that account for signal propagation decays is known to be a very complex, challenging problem. For analytic tractability, researchers, when addressing high-layer related issues, often use the 0-1 interference model where signals are assumed to cause interference only when they are received within a distance threshold or a transmission range. In this interference model, the amount of interference does not depend on the distances from the interfering sources. Clearly, this model cannot reflect, nor capture all dynamics of real wireless environments. In a real environment, the amount of interference depends on signals' strengths, which in turn depend on distances from the sources of interfering signals, and hence, so does MIMO's ability to suppress interference. Although such a model may not be accurate enough to be used for studying physical-layer performances of point-to-point, MIMO links, it can be used as an abstraction for studying high-layer performances. The 0-1 model can still provide useful insights and characterization of high-layer network performances, such as providing upper bounds on the multi-hop network throughput. In this work, we use the 0-1 model to characterize each link with a constant data rate, which can, for example, signify the link's average, minimum, or maximum achievable data rate. By setting the transmission range to the distance that provides the highest data rate, the 0-1 model can then be used to characterize upper bounds on links' data rates. In essence, although this model is relatively simple, it can still provide useful characterization of how the total throughput behaves in multi-hop networks, as will be shown in this paper.

[2]Note that we only provide key features of the models relevant to this work. Hence, we omit details of how and when nodes exchange such information as weight vectors.

F. Effective Degrees of Freedom

Based on the illustrations given in Section II-B, one can draw the following conclusion. A node's degrees of freedom (DoFs) or number of antennas can be exploited in one of the following three ways: (1) all DoFs are used to send a multiple-stream flow of data by exploiting the spatial division multiplexing of the antenna array; (2) all DoFs are used to increase the spatial reuse of the spectrum by allowing multiple concurrent streams in the same vicinity; (3) some of DoFs are used to send a multiple-stream flow while the others are used to allow for concurrent streams in the same neighborhood. It is important to note that the level of exploitation of the spatial reuse and/or multiplexing is, however, contingent on physical limitations, such as nodes' power availabilities, multipath conditions, channel correlation, and/or channel estimation errors.

Therefore, when a node is equipped with γ antennas, it does not mean that γ concurrent streams (spatial reuse and/or multiplexing) can occur within the node's vicinity; physical limitations may restrict the number of possible concurrent streams to be less than γ. Let's consider two neighbor nodes m and n each equipped with an antenna array of size γ_m and γ_n, respectively, and assume that m wants to transmit a χ-stream data signal to n. Suppose there are φ streams currently being received by nodes located within m's transmission range, and ψ streams currently being transmitted by nodes located within n's reception range. Due to physical limitations, the number $(\varphi + \chi)$ of possible concurrent streams in m's vicinity is likely to be less than the number of its actual antenna elements γ_m [22]. We will refer to this number $\alpha_m = (\varphi + \chi)$ as *effective transmit degrees of freedom* of node m. For similar reasons, the number $(\psi + \chi)$ of possible concurrent streams in n's vicinity is also likely to be less than its total number of antennas γ_n [22]. This number $\beta_n = (\psi + \chi)$ will be referred to as *effective receive degrees of freedom* of node n.

It is important to note that these effective (both transmit α_m and receive β_n) DoFs can be viewed as cross-layer models that capture the effects of the physical limitations, such as power level, channel correlation, and channel estimation, on the transmission and reception capabilities of multi-antenna systems. For example, a node equipped with 10 antennas may only be capable of having 6 or 5 concurrent streams within its vicinity due to the correlation between channel coefficients or due to errors associated with its channel estimation method. In [23], we derived a statistical method that allows each node m to determine both α_m and β_m given these network's physical limitations. In this paper, we assume that these two numbers are known for each node by using this method.

We will use these numbers to model radio and interference constraints, which will, in turn, be used to formulate the end-to-end network throughput problem. Therefore, the effects of physical limitations on throughput performance will be accounted for by incorporating these cross-layers models into throughput formulations as will be described next.

III. Problem Statement

In this paper, we want to characterize and analyze the maximum achievable throughput in multi-hop wireless networks equipped with MIMO links. We propose and analyze three different MIMO protocols—spatial reuse only protocol (SRP), spatial multiplexing only protocol (SMP), and spatial reuse & multiplexing protocol (SRMP)—all of which increase network throughput, but each with a different way of exploiting the multiple antenna benefits.

Spatial Reuse Only MIMO Protocol (SRP): uses all effective degrees of freedom to increase network throughput via spatial reuse of the spectrum only. In SRP, the throughput is then increased by allowing multiple simultaneous communication sessions in the same neighborhood.

Spatial Multiplexing Only MIMO Protocol (SMP): under which all effective degrees of freedom are used to increase throughput via spatial multiplexing only. Nodes in SMP can use their multiple antennas to communicate multiple stream signals among them. They cannot, however, use any of their effective degrees of freedom to increase spatial reuse.

Spatial Reuse & Multiplexing MIMO Protocol (SRMP): is a combination of SRP and SMP in that the effective degrees of freedom can be used to increase network throughput via spatial reuse and/or spatial multiplexing, whichever provides higher throughput.

In this paper, we consider TDMA (Time Division Multiplexing Access), in which time is divided into slots of an equal length, denoted by $T = \{1, 2, \ldots\}$. Characterizing the achievable throughput under TDMA will then serve as a characterization of the throughput achievable under other multiple access methods, such as CDMA and CSMA/CA.

For each MIMO protocol, we formulate the multi-hop routing problem as a standard multi-commodity flow instance that consists of a set Q of commodities where each $q \in Q$ is characterized with a source-destination pair $s(q), d(q)$ of nodes, and a non-negative multi-hop flow of rate f_q. A multi-hop flow solution—maximizing the sum $\sum_{q \in Q} f_q$ of all flows' rates subject to the network constraints that we will describe and model in next sections—will be used to represent the achievable throughput under multi-commodity flow $f = (f_q)_{q \in Q}$. By solving many instances, we can provide a statistical characterization and analysis of the maximum achievable throughput in multi-hop wireless MIMO networks.

Our main contributions are two-fold. First, we characterize and analyze the optimal achievable throughput in multi-hop wireless networks that are equipped with MIMO links. We also study the effects of several network parameters on this throughput. Second, we show how the thus-obtained results can be used for designing wireless MIMO networks such as MIMO mesh networks. These results enable network designers to determine the optimal parameters of wireless MIMO networks.

IV. Model

A. Signal Propagation Assumptions

Signals in reality decay gradually with distance, and deriving models and constraint designs that mimic interference while accounting for such a decay is too difficult to do, especially in multi-hop settings. Therefore, we assume a 0-1 model, where signals can cause interference only when

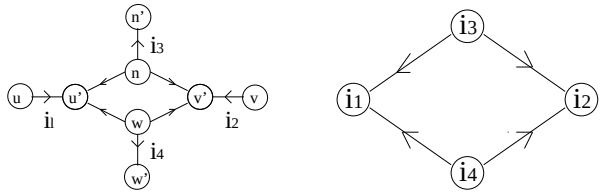

(a) $G = (N, L)$ (b) $H = (L, C)$

Fig. 3. (a) node topology graph, (b) link interference graph

received within a distance threshold or a transmission range, i.e., signals can either interfere with each other, or not at all. This model can still be used (and has been used in many other efforts) as an abstraction for providing upper bounds on the end-to-end network throughput. Note that the 0-1 model can be viewed as characterization/association of a link with a constant data rate (it can, for example, signify the link's average, minimum, or maximum achievable data rate), whereas the decaying model can be viewed as characterization of a link with a variable (e.g., instantaneous) data rate. By defining/setting the transmission range as the distance which provides the highest data rate, the 0-1 model can then be used to characterize upper bounds on links' data rates. Since our goal is to characterize upper bounds on end-to-end throughput of multi-hop networks, the 0-1 model can still provide useful characterization of how the total network throughput behaves.

B. Network Model

We model the multi-hop wireless MIMO network as a directed graph $G = (N, L)$, referred to as *node topology graph*, with a finite nonempty set N of nodes and a finite set L of MIMO links. L is the set of all ordered pairs (m, n) of distinct nodes in N such that n is within m's transmission range. If $i = (m, n) \in L$, then node m and node n are referred to as the transmitter $t(i)$ and the receiver $r(i)$ of link i. A data link i is said to be *active* if $t(i)$ is currently transmitting to $r(i)$; otherwise, i is said to be *inactive*. For every $m \in N$, let $L_m^+ = \{i \in L : t(i) = m\}$ denote the set of all links whose transmitter is m, $L_m^- = \{i \in L : r(i) = m\}$ denote the set of all links whose receiver is m, and $L_m = L_m^+ \cup L_m^-$. Fig. 3(a) shows an example of node topology graph. We assume that each node m is equipped with an antenna array of γ_m elements that it uses to transmit and receive signals, and we let α_m and β_m denote node m's effective transmit and receive degrees of freedom. For every $i \in L$, let c_i denote the maximum number of bits that link i can support in one second. While c_i depends on i (i.e., could vary from link to link), it is assumed to be time-invariant.

Let C denote the set of all ordered distinct pairs $(i, j) \in L \times L$ such that (1) i and j do not share a node between them and (2) the transmission on link i interferes with the reception on link j. Note that if $(i, j) \in C$, it does not necessarily mean that $(j, i) \in C$. We now model the multi-hop wireless MIMO network as a directed graph $H = (L, C)$, which we will refer to as a *link interference graph*. The graph H corresponding to the node topology graph G given in Fig. 3(a) is shown in Fig. 3(b) for illustration. Given a link $i \in L$, let $C_i^+ = \{j \in L : (i, j) \in C\}$ denote the set of all links whose receivers are interfered by the transmission on i, and $C_i^- = \{j \in L : (j, i) \in C\}$ denote the set of all links whose transmitters are interfered by the reception on i. Referring to the example in Fig. 3(b), $C_{i_3}^+ = \{i_1, i_2\}$ and $C_{i_1}^- = \{i_3, i_4\}$.

V. Constraint Design and Modeling

In this section, we model the packet-level constraints on multi-hop wireless MIMO networks, described in Section IV. For every $(i, t) \in L \times T$, we define the binary variable y_i^t to be 1 if link i is active during time slot t, and 0 otherwise. We now consider each of the three MIMO protocols: SRP, SMP, and SRMP.

A. Spatial Reuse Only MIMO Protocol (SRP)

1) Radio Constraints: Due to radio limitations, we assume that a node can either transmit or receive, but not both, at a time slot. Also, since SRP exploits all degrees of freedom (DoFs) to increase spatial reuse, a node can use at most one DoF to transmit or receive one stream while the other DoFs can be used to allow for multiple concurrent streams in same vicinities. Hence, one can write

$$\textstyle\sum_{i \in L_m} y_i^t \leq 1, \quad \forall m \in N, \forall t \in T. \tag{1}$$

2) Interference Constraints: Next, we describe the interference constraints under both the non-cooperative interference avoidance model (NiM) and the cooperative interference avoidance model (CiM), as defined in Section II-D.

Interference Constraints under NiM: Recall that under NiM, receivers must be responsible for suppressing signals from interfering transmitters. Hence, any receiver must have enough effective receive degrees of freedom that enable it to combat nearby transmitters' interference prior to receiving a signal at any time slot. That is, $\forall i \in L$ and $\forall t \in T$,

$$(\omega - \beta_{r(i)} + 1) y_i^t + \textstyle\sum_{j \in C_i^-} y_j^t \leq \omega \tag{2}$$

where ω is an integer larger than the maximum number of active links at any given time slot. Let $\omega = |L|$. If $y_i^t = 1$ (i.e., i is active at time slot t), then the above constraints ensure that the total number of active links, interfering with the reception on link i, does not exceed what node $r(i)$'s effective receive degrees of freedom can handle; otherwise (if $y_i^t = 0$), the constraints are relaxed since i is not active, and hence, no interference needs to be suppressed.

Likewise, transmitters under NiM must also be responsible for nulling their signals at all nearby receivers. That is, prior to transmission at any time slot, a transmitter must have enough effective transmit degrees of freedom so that it can prevent its signal from causing interference to any nearby receivers. Hence, we can write, for all $i \in L$ and all $t \in T$,

$$(\omega - \alpha_{t(i)} + 1) y_i^t + \textstyle\sum_{j \in C_i^+} y_j^t \leq \omega. \tag{3}$$

Again, the above constraints ensure that the maximum number of active links interfering with the transmission on link i does not exceed what node $t(i)$ can null, i.e., no more than $\alpha_{t(i)}$ can be concurrently active at time slot t when i is active. If, however, $t(i)$ is not transmitting (i.e., $y_i^t = 0$), then the

constraints are relaxed as expressed by the inequality via ω.

Interference Constraints under CiM: Under CiM, for every pair $(i,j) \in C$, one of the following two conditions must hold: the transmitter of i must null its signal at the receiver of j; or the receiver of j must suppress the interference from the transmission on link i. Note that one (and only one) of the above two conditions needs to hold for a successful transmission on i while still receiving an interference-free signal on j. To express this set of constraints, we need to introduce two new binary variables. For every $t \in T$ and for every $(i,j) \in C$, we define binary variables

$$\lambda_{ij}^t = \begin{cases} 1 & \text{if } i \text{ and } j \text{ are both active at } t, \text{ and } t(i) \\ & \text{nulls its signal at } r(j) \\ 0 & \text{otherwise} \end{cases}$$

and binary variables

$$\mu_{ij}^t = \begin{cases} 1 & \text{if } i \text{ and } j \text{ are both active at } t, \text{ and } r(j) \\ & \text{suppresses the interference from } t(i) \\ 0 & \text{otherwise.} \end{cases}$$

The interference constraints to SRP under CiM can then be expressed as follows. For all $(i,j) \in C$ and all $t \in T$,

$$\begin{cases} 1 + \sum_{l \in C_i^+} \lambda_{il}^t \leq \alpha_{t(i)} \\ 1 + \sum_{l \in C_j^-} \mu_{lj}^t \leq \beta_{r(j)} \\ y_i^t + y_j^t \leq \lambda_{ij}^t + \mu_{ij}^t + 1. \end{cases} \quad (4)$$

It is important to note that when the number of antennas equals 1 ($\gamma_m = 1,\ \forall m \in N$), the interference constraints under NiM (Eqs. (2) and (3)) are equivalent to those under CiM (Eqs. (4)). This claim can easily be proven; it will also be justified in the evaluation section via simulations (Section VII-C).

B. Spatial Multiplexing Only MIMO Protocol (SMP)

This section describes and models the packet-level (radio and interference) constraints under SMP.

1) Radio Constraints: Recall that SMP exploits all DoFs to increase data rates/throughput by allowing transmitter-receiver pairs to communicate multiple stream signals over their links, i.e., each transmitter-receiver pair, $(t(i), r(i))$, can communicate more than one stream over link i. Let z_i^t represent the number of streams that are active on link i at time slot t. Because the maximum number of streams communicated on link i must not exceed the effective transmit degrees of freedom of $t(i)$ nor the effective receive degrees of freedom of $r(i)$,

$$z_i^t \leq \alpha_{t(i)} y_i^t \text{ and } z_i^t \leq \beta_{r(i)} y_i^t \quad (5)$$

must hold $\forall i \in L$ and $\forall t \in T$. Like in SRP, in SMP, a node can either transmit or receive at any given time slot, and can at most be active on one link. Hence, the constraints in Eq. (1) must also hold under SMP; i.e.,

$$\sum_{i \in L_m} y_i^t \leq 1, \quad \forall m \in N, \forall t \in T. \quad (6)$$

2) Interference Constraints: Recall that all DoFs in SMP are used for spatial multiplexing, i.e., none of them are exploited to increase spatial reuse. Therefore, NiM and CiM are equivalent under SMP, and so are the interference constraints. These constraints can be written as

$$y_i^t + y_j^t \leq 1, \forall (i,j) \in C, \forall t \in T. \quad (7)$$

C. Spatial Reuse & Multiplexing MIMO Protocol (SRMP)

We now describe and model the packet-level constraints under SRMP. Note that the radio constraint under SRMP are equivalent to those under SMP as described in Section V-B.1. The interference constraints, however, are different from those under SRP or SMP.

Interference Constraints under NiM: Under NiM, receivers are responsible for suppressing signals from interfering transmitters, i.e., for all $i \in L$ and all $t \in T$,

$$(\Omega - \beta_{r(i)}) y_i^t + \sum_{j \in C_i^- \cup L_{r(i)}^-} z_j^t \leq \Omega \quad (8)$$

and transmitters are responsible for nulling their signals at all nearby receivers, i.e., for all $i \in L$ and all $t \in T$,

$$(\Omega - \alpha_{t(i)}) y_i^t + \sum_{j \in C_i^+ \cup L_{t(i)}^+} z_j^t \leq \Omega \quad (9)$$

where Ω is an integer greater than the number of possible concurrent streams. Let $\Omega = |L| \times \max_{m \in N} \gamma_m$.

Interference Constraints under CiM: For every $(i,j) \in C$ and for every $t \in T$, we introduce two integer variables, θ_{ij}^t and ϑ_{ij}^t. θ_{ij}^t represents the number of DoFs assigned by $t(i)$ to null its signal at $r(j)$, provided both i and j are active, i.e., $r(j)$ can have up to θ_{ij}^t interference-free streams. ϑ_{ij}^t represents the number of DoFs assigned by $r(j)$ to suppress interference coming from $t(i)$, provided both i and j are active, i.e., ϑ_{ij}^t streams can be sent by $t(i)$ without causing interference at $r(j)$. The constraints under CiM can then be written as follows. For all $(i,j) \in C$ and all $t \in T$,

$$\begin{cases} \sum_{l \in L_{t(i)}^+} z_l^t + \sum_{l \in C_i^+} \theta_{il}^t \leq \alpha_{t(i)}, \\ \sum_{l \in L_{r(j)}^-} z_l^t + \sum_{l \in C_j^-} \vartheta_{lj}^t \leq \beta_{r(j)}, \\ z_i^t \leq \vartheta_{ij}^t + \alpha_{t(i)}(1 - y_i^t), \\ z_j^t \leq \theta_{ij}^t + \beta_{r(j)}(1 - y_j^t). \end{cases} \quad (10)$$

D. Observations

There are two points worth mentioning regarding the above design constraints. First, they all constrain the feasibility of data transmissions on a packet-by-packet basis. That is, at every time slot, packet-level conditions must all be met in order for packet transmissions to be successful during that time slot; these constraints can then be seen as conditions under which the *instantaneous* link rates are feasible. Second, they all are necessary conditions, but not sufficient for the feasibility of packet transmissions. That is, if, at a given time slot t, some or all of these constraints are not met, then some or all of the packets transmitted at time t will be unsuccessful, whereas meeting all of these constraints does not guarantee successful transmissions of all packets.

VI. Maximum Multi-commodity Flow

A. LP Relaxations: Flow-Level Design

There are two subtle issues with the packet-level constraints described in Section V. First, they are expressed in integer variables. Hence, the multi-commodity flow formulation described in Section III cannot be solved by the standard linear programming. Second, they are instantaneous, i.e., at every time slot, there is a set of constraints that must be met. This will increase the size of the optimization problem in terms of the number of constraints as well as variables.

We want to provide LP relaxations of these constraints to address the above two issues. As it will become clear shortly, the relaxed constraints can be seen as necessary conditions on the feasibility of *average* link rates. Note that, by definition, LP relaxations result in widening the feasibility space; that is, the solutions obtained under the average-rate (relaxed) constraints may be infeasible under the instantaneous-rate constraints. However, since we aim to characterize the maximum achievable throughput, these relaxations will only make the maximum less tight. Clearly, there is a tradeoff between the quality of solutions and the size/complexity of problems. To keep the problem simple while drawing useful conclusions, we choose to work with the relaxed constraints instead of the packet-level ones. Next we provide LP relaxations to the packet-level constraints described in the previous section.

Let's consider a set of time slots $S \subseteq T$ of cardinality τ, and for all $i \in L$, define y_i to be $\frac{1}{\tau}\sum_{t\in S} y_i^t$. For every $(i,j) \in C$, let $\lambda_{ij} = \frac{1}{\tau}\sum_{t\in S}\lambda_{ij}^t$ and $\mu_{ij} = \frac{1}{\tau}\sum_{t\in S}\mu_{ij}^t$. Note that y_i represents the fraction of time in S during which link i is active; λ_{ij} represents the fraction of time in S during which links i and j are both active and $t(i)$ is nulling its signal at $r(j)$; and μ_{ij} represents the fraction of time in S during which links i and j are both active and $r(j)$ is suppressing the interference caused by $t(i)$'s signal.

For every $i \in L$, we also define the continuous variables z_i as $\frac{1}{\tau}\sum_{t\in S} z_i^t$, and for all $(i,j) \in C$, let $\theta_{ij} = \frac{1}{\tau}\sum_{t\in S}\theta_{ij}^t$ and $\vartheta_{ij} = \frac{1}{\tau}\sum_{t\in S}\vartheta_{ij}^t$. Suppose that $i,j \in L$ are both active during S. Here, z_i represents the average number of streams that are active on link i during S; θ_{ij} represents the average number of effective transmit degrees of freedom that $t(i)$ allocates to null its signal at $r(j)$; and ϑ_{ij} represents the average number of effective receive degrees of freedom that $r(j)$ allocates to suppress the interference coming from $t(i)$. Recall that all these continuous variables are *averages* over the length of the time slot set S. Hence, the longer S is, the more accurate these averages are. We assume that S is long enough for these variables to reflect accurate averages.

By using these continuous variables, one can provide LP relaxations to the packet-level constraints described in Section V. For example, by summing both sides of Eq. (1) over S and interchanging summations between i and t, one can obtain $\sum_{i\in L_m} y_i \le 1, \forall m \in N$. Likewise, one can obtain LP relaxations of all the packet-level (or instantaneous) constraints described in Section V. For convenience, we summarize all the obtained LP relaxation constraints in Table I (under SRP), Table II (under SMP), and Table III (under SRMP).

TABLE I

LP relaxation constraints under SRP

SRP/Radio:	$\sum_{i\in L_m} y_i \le 1, \forall m \in N$	
SRP/NiM:	$(\omega - \beta_{r(i)} + 1)y_i + \sum_{j\in C_i^-} y_j \le \omega,$ $(\omega - \alpha_{t(i)} + 1)y_i + \sum_{j\in C_i^+} y_j \le \omega,$	$\forall i \in L$
SRP/CiM:	$1 + \sum_{l\in C_i^+}\lambda_{il} \le \alpha_{t(i)},$ $1 + \sum_{l\in C_j^-}\mu_{lj} \le \beta_{r(j)},$ $y_i + y_j \le \lambda_{ij} + \mu_{ij} + 1,$	$\forall (i,j) \in C.$

TABLE II

LP relaxation constraints under SMP

SMP/Radio:	$\sum_{i\in L_m} y_i \le 1, \forall m \in N$ $z_i \le \alpha_{t(i)} y_i,$ $z_i \le \beta_{r(i)} y_i,$	$\forall i \in L$
SMP/NiM and SMP/CiM: $y_i + y_j \le 1, \forall (i,j) \in C$		

B. LP Formulation

Let's consider a multi-hop wireless MIMO network routing instance that consists of a set Q of commodities, and let x_i^q denote link i's data rate that belongs to commodity q. Note that the flow-balance constraints,

$$\sum_{j\in L_{t(i)}^+} x_j^q = \begin{cases} f_q & \text{if } t(i) = s(q) \\ \sum_{j\in L_{t(i)}^-} x_j^q & \text{Otherwise,} \end{cases} \tag{11}$$

must be satisfied for all $q \in Q$ and all $i \in L$. By letting

$$\frac{1}{c_i}\sum_{q\in Q} x_i^q = \begin{cases} y_i & \text{if under SRP} \\ z_i & \text{if under SMP or SRMP} \end{cases} \tag{12}$$

for all $i \in L$, the multi-hop wireless MIMO network routing problem can be formulated as a standard LP whose objective is to maximize $\sum_{q\in Q} f_q$ subject to the flow-balance constraints given in Eqs. (11) and (12), and the radio and interference constraints given in Table I (under SRP), Table II (under SMP), or Table III (under SRMP).

VII. Throughput Characterization

In this section, we use extensive simulations to characterize and analyze the end-to-end throughput that multi-hop wireless MIMO networks can achieve under the three MIMO protocols (SRP, SMP, and SRMP), and for the two interference avoidance models (NiM and CiM). We generate random multi-hop wireless MIMO networks, each consisting of `N` nodes. We set the medium's capacity, defined to be the maximum number of bits that a node with one antenna can transmit in one second, to unity ($c_i = 1, \forall i \in L$), and assume that all nodes are equipped with the same number of antennas ($\gamma_m = \gamma, \forall m \in N$). Nodes are uniformly distributed in a $100m \times 100m$ square where two nodes are considered neighbors if the distance between them does not exceed `TxRange` meters. For each random network, `Q` source-destination pairs are randomly generated to form `Q` end-to-end multi-hop commodity flows. Each LP formulation (SRP/NiM, SRP/CiM, SMP/NiM, SMP/CiM, SRMP/NiM, and SRMP/CiM), defined in Section VI, is solved for each

TABLE III
LP RELAXATION CONSTRAINTS UNDER SRMP

SRMP/Radio:	$\sum_{i \in L_m} y_i \leq 1, \forall m \in N$ $z_i \leq \alpha_{t(i)} y_i,$ $z_i \leq \beta_{r(i)} y_i,$	$\forall i \in L$
SRMP/NiM:	$(\Omega - \beta_{r(i)}) y_i + \sum_{j \in C_i^- \cup L_{r(i)}^-} z_j \leq \Omega,$ $(\Omega - \alpha_{t(i)}) y_i + \sum_{j \in C_i^+ \cup L_{t(i)}^+} z_j \leq \Omega,$	$\forall i \in L$
SRMP/CiM:	$\sum_{l \in L_{t(i)}^+} z_l + \sum_{l \in C_i^+} \theta_{il} \leq \alpha_{t(i)},$ $\sum_{l \in L_{r(j)}^-} z_l + \sum_{l \in C_j^-} \vartheta_{lj} \leq \beta_{r(j)},$ $z_i \leq \vartheta_{ij} + \alpha_{t(i)}(1 - y_i),$ $z_j \leq \theta_{ij} + \beta_{r(j)}(1 - y_j).$	$\forall (i,j) \in C$

network to find the maximum achievable throughput. All simulations are run until the measured throughput converges to within 5% of real values at a 98% confidence level.

A. Evaluation Parameters

In this work, we study the effects of the following network parameters on the maximum achievable network throughput.

a) Transmission range (`TxRange`*):* Recall that the higher the transmission range, the greater the interference, but also the higher the node degree. Typically, a higher interference results in less throughput, while a higher node degree yields more throughput. Here, we want to see if this trend holds even when nodes are equipped with MIMO links, and if so, to what extent it does. In this study, we fix `N` to 50 and `Q` to 25, and vary `TxRange` from $16m$ to $32m$.

b) Node density (`NodeDensity`*):* Like the transmission range case, the higher the node density, the greater the node degree, and hence, the higher the throughput (provided other network parameters are kept the same). Unlike the transmission range case, increasing the node density while keeping the same number of commodities does not, however, raise interference levels. In this study, we want to see how sensitive throughput is to node density when MIMO sizes are varied. Here, we fix `TxRange` to $30m$ and `Q` to 10, and vary `NodeDensity` from 0.2% to 0.5% (by varying `N` from 20 to 50).

c) Multi-hop length (`HopLength`*):* So far, `Q` source-destination pairs are generated randomly, and hence, so are their hop lengths (average hop length varied between 2.74 for `TxRange` $= 32m$ and 8.27 for `TxRange` $= 16m$). Here, we study the effect of hop length on the achievable throughput. In order to mask the effects of other network parameters, we consider a mesh network of `N` $= 50$ nodes where each node has exactly 4 neighbors. In all simulation runs, we set the number `Q` of commodity flows to 25. We consider 5 different hop lengths: 1, 3, 5, 7, and 9 hops. For each `HopLength`, we generate and simulate random sets, each of `Q` flows whose lengths are all `HopLength` hops.

The maximum achievable throughput, shown in each graph presented in this section, signifies the per-commodity flow throughput calculated as the average end-to-end throughput over all the `Q` commodity flows.

B. Throughput Characterization and Analysis under NiM

We first study and analyze the network throughput behavior under NiM for each of the three MIMO protocols: SRP, SMP, and SRMP. Then, in Section VII-C, we study this same behavior under CiM, and compare it with that observed under NiM.

1) Study of SRP: Fig. 4 shows the effect of transmission range (Figs. 4(a) and 4(d)), node density (Figs. 4(b) and 4(e)), and hop length (Figs. 4(c) and 4(f)) on the achievable throughput under SRP.

a) The asymptotic bound: Figs. 4(a), 4(b), and 4(c) show that regardless of transmission range, node density, and/or hop length, as the number of antennas increases, the maximum achievable throughput first rises and then flattens out asymptotically. This can be explained as follows. Recall that multiple antennas increase spatial reuse by allowing multiple simultaneous communication sessions in the same vicinity, i.e., nodes can, for example, use their antennas to suppress the undesired signals sent by nearby transmitters, allowing them to receive interference-free signals concurrently with nearby transmitted signals. Therefore, one may conclude that the more antennas a node has, the more nearby transmitters' signals it can suppress, and hence, the higher throughput the network can achieve. Because, in a given network, each node (e.g., receiver) has a fixed number of interfering nodes (e.g., nearby transmitters), increasing the size of the antenna array beyond that fixed number of interfering nodes cannot increase the network throughput any further since spatial reuse can no longer be increased even if more antennas are added. This is why we see an asymptotic bound on the achievable throughput under SRP.

b) Effect of transmission ranges—the interference-path diversity tradeoff: Fig. 4(a) shows that for small numbers of antennas, the higher the transmission range, the less the achievable throughput. Conversely, when there are a large number of antennas, the higher the transmission range, the greater the throughput. Also, Fig. 4(d) indicates that as the transmission range increases, the achievable throughput always decreases when each node is equipped with a single antenna. In contrast, the throughput first increases and then decreases when each node is equipped with multiple antennas—for each MIMO size, there exists a transmission range that maximizes the achievable throughput. Note that this optimal transmission range increases as the number of antennas increases. Recall that in networks with long transmission ranges, nodes are likely to have more neighbors. While this provides nodes with higher path diversity, it also provides them with more interference to combat. Hence, when transmission ranges are long, interference dominates if nodes are only equipped with single or small-sized antenna arrays which are not enough to combat the extra interference caused by the long ranges of transmission, thereby achieving less overall throughput. When the number of antennas is large enough, nodes can, however, take advantage of the increased number of paths to find better routes while effectively combating the interference by using their antennas.

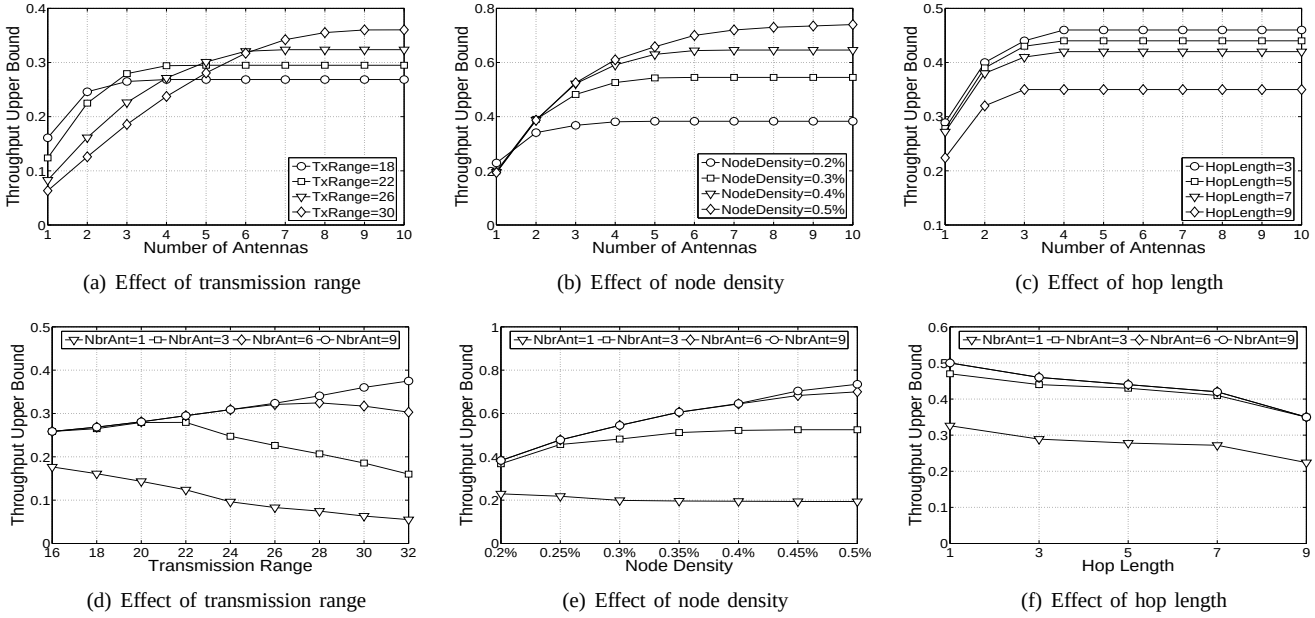

(a) Effect of transmission range (b) Effect of node density (c) Effect of hop length

(d) Effect of transmission range (e) Effect of node density (f) Effect of hop length

Fig. 4. Maximum achievable throughput under SRP.

In this case, the throughput will be increased as more concurrent communication sessions are enabled in the same vicinity. This explains why for a large number of antennas, the achievable throughput for long transmission ranges are greater than those for short transmission ranges.

c) Effect of node density—path diversity at no interference cost: An increase in node density typically yields path diversity as it raises the number of possible end-to-end paths. If the number Q of commodity flows is kept the same as in our case, such an increase in node density does not incur extra interference. When the number of antennas is small (1 or 2, see Fig. 4(b)), path diversity cannot be exploited to increase network throughput. This is because even when presented with more paths to route through, nodes do not have enough antennas to suppress interference at each of those neighboring nodes involved in their multi-path routes. This is why the throughput achievable under small antennas sizes does not depend on node density as shown in Fig. 4(b). When the number of antennas is large, the throughput achievable in dense networks is, however, greater than that in sparse networks due to the multi-path nature arising from higher node degrees; nodes can use their antennas to suppress interference at the nearby nodes involved in multi-path routes while still exploiting path diversity to increase throughput.

For each multiple antenna case, Fig. 4(e) shows that there exists a node density beyond which the achievable network throughput can no longer increase. In other words, for a given set of commodity flows, there is a certain node density threshold beyond which network throughput cannot be increased even if nodes are provided with more paths to route through.

d) Effect of hop length: Figs. 4(c) and 4(f) indicate that irrespective of the number of antennas, the larger the hop length of end-to-end flows, the less overall network throughput. This is because multi-hop flows with high multiplicity tend to create greater contention for, and hence more interference in, the wireless medium than those with small hop multiplicity. That is, the longer the multi-hop paths, the more flows a node is likely to forward traffic for, and hence, the more contention and interference nodes are likely to deal with.

2) Study of SMP: Fig. 5 shows the effect of transmission range (5(a) and 5(d)), node density (5(b) and 5(e)), and hop length (Figs. 5(c) and 5(f)) on the maximum achievable throughput under SMP. These figures indicate that regardless of transmission range, node density, and/or hop length, the maximum achievable throughput increases almost linearly as a function of the number of antennas. Unlike SRP, under SMP, the number of signals' streams is proportional to the number of antennas, and hence, so is the overall network throughput, thus making a linear increase in network throughput.

Fig. 5(d) shows that the achievable throughput decreases as the transmission range increases, and this holds regardless of the size of the antenna array. This decline in throughput is due to the fact that the excess of interference resulting from the increase in the transmission range cannot be suppressed under SMP even when nodes are equipped with many antennas; under SMP, all antennas are exploited to increase data rates instead of combating interference. Fig. 5(e) shows that regardless of the number of antennas, the achievable throughput also decreases as the hop length increases. This is because the increase in flows' number of hops introduces extra interference that SMP cannot suppress, either. Unlike the transmission range and hop length cases, throughput does not depend on node density, given a fixed size of antenna array. This is simply because an increase in node density does not incur extra interference.

3) Study of SRMP: Fig. 6 shows the effect of transmission range (6(a) and 6(d)), node density (6(b) and 6(e)), and hop length (Figs. 6(c) and 6(f)) on the maximum achievable throughput under SRMP. First, note that the achiev-

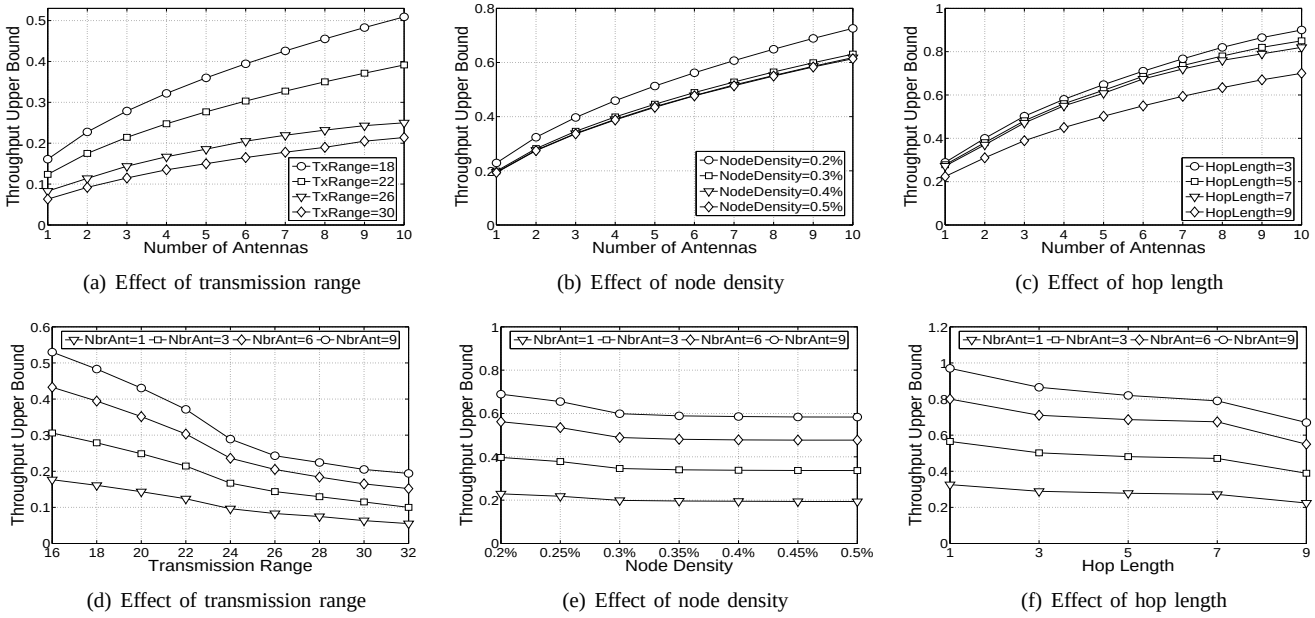

(a) Effect of transmission range (b) Effect of node density (c) Effect of hop length

(d) Effect of transmission range (e) Effect of node density (f) Effect of hop length

Fig. 5. Maximum achievable throughput under SMP.

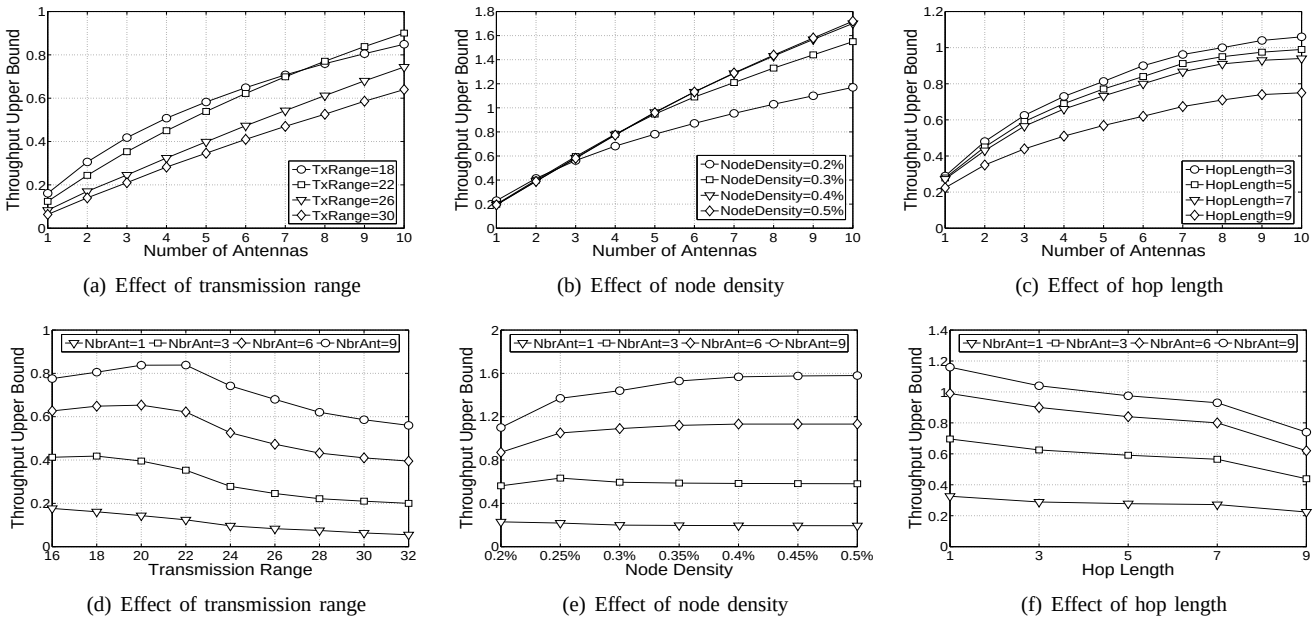

(a) Effect of transmission range (b) Effect of node density (c) Effect of hop length

(d) Effect of transmission range (e) Effect of node density (f) Effect of hop length

Fig. 6. Maximum achievable throughput under SRMP.

able throughput under SRMP increases almost linearly as a function of the number of antennas for all combinations of transmission range, node density, and hop length. Recall that SRMP combines both SRP and SMP in that it increases network throughput via spatial reuse and/or spatial multiplexing, whichever provides more overall throughput. As a result, when antennas can no longer be exploited to increase throughput via spatial reuse (i.e., when throughput gained via SRP flattens out), SRMP can still exploit the antennas to increase network throughput further by achieving higher data rates via spatial multiplexing.

4) Design Guidelines: There is an important and useful trend that one can observe from the results presented in this section: For a given combination of a MIMO size and a node density, there exists an optimal transmission range that maximizes the achievable network throughput (see Fig. 4(d) for SRP, and Fig. 6(d) for SRMP). Similarly, for a given combination of a MIMO size and a transmission range, there is a certain node density threshold beyond which throughput can no longer be increased (see Fig. 4(e) for SRP, and Fig. 6(e) for SRMP). Fig. 7 shows these optimal transmission ranges (Fig. 7(a)) and node densities (Fig. 7(b)) for several MIMO sizes. Note that both the optimal transmission range and the optimal node density increase with the number of antennas. Also, observe that when the number of antennas is large, these optima are higher under SRP than under SRMP. An explanation of this trend is already provided in Section VII-B.1.

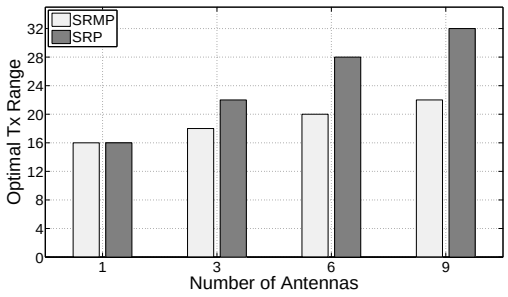

(a) Optimal transmission range: $\texttt{NodeDensity} = 0.5\%$

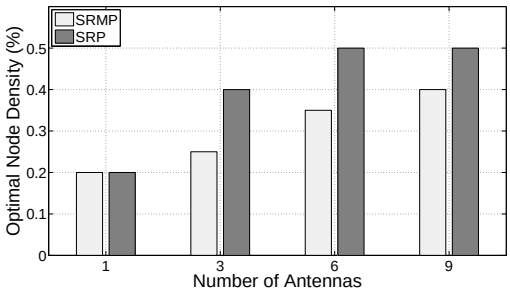

(b) Optimal node density: $\texttt{TxRange} = 30m$

Fig. 7. Optimal design parameters under SRP and SRMP.

Therefore, this study can provide guidelines for network designers to determine optimal parameters for wireless MIMO networks; it can be used to determine optimal transmission ranges and node densities of wireless MIMO-equipped networks. MIMO-equipped mesh networks are an example where this study can be very useful. For instance, knowing the size of antenna arrays of mesh nodes, a network designer can use this study to determine the optimal mesh node density (i.e., optimal number of mesh nodes) and the optimal transmission range (i.e., optimal transmission power) that maximize the total network throughput.

C. Throughput Characterization and Analysis Under CiM: Non-cooperative vs. Cooperative Interference Avoidance

In this section, we study and characterize the optimal throughput that multi-hop MIMO networks can achieve under CiM. Because the behaviors and trends of the throughput achievable under CiM are found similar to those achievable under NiM, which we already discussed and presented in Section VII-B, we focus here on providing a comparative analysis between CiM and NiM.

Fig. 8 shows the maximum achievable throughput under NiM and CiM. Note that because NiM and CiM are equivalent under SMP, we only show the results under SRP and SRMP. From the figures, we observe that when nodes are equipped with single antennas, the throughput achievable under NiM is identical to that achievable under CiM. As expected and already discussed in Section V-A, this means that cooperation does not provide more throughput when nodes are not equipped with multiple antennas. Likewise, one can observe that when the number of antennas is large, the achievable throughput tends to be the same regardless of whether the nodes cooperate. As explained earlier, this is because when a node has a large number of antennas, it can combat interference by itself even in the absence of cooperation among nodes. It is when the number of antennas is not large enough to suppress all interference that cooperation can increase throughput. When nodes cooperate, redundant interference suppression can be avoided, thus allowing more concurrent communications. In this case, CiM provides greater throughput than NiM. For example, if a transmitter interferes with a nearby undesired receiver, then both the transmitter and the receiver may each end up using one of its antennas to avoid interference when they do not cooperate. When both the transmitter and the receiver cooperate as under CiM, one of them can use one of its antennas to avoid the interference while the other node can use its antenna to avoid interference with another interfering node, thereby increasing the spatial reuse.

D. Spatial Reuse vs. Spatial Multiplexing

We now compare the performances of SRP and SMP against each other (SRMP always outperforms the other two). (Here, we only show the results obtained under NiM since both NiM and CiM give similar behaviors). Figs. 9, 10, and 11 show the throughput achievable under all MIMO protocols for different values of transmission ranges, node densities, and hop lengths. First, as expected, when nodes are equipped with single antennas, the achievable throughput is identical under all protocols, regardless of transmission ranges, node densities, and/or hop lengths.

Second, when transmission ranges are short (Fig. 9(a)) or node densities are low (Fig. 10(a)), SMP achieves higher network throughput than that achievable under SRP. However, when transmission ranges or node densities are high, the exact opposite trend is observed. In fact, as the transmission range and/or the node density increase, the throughput achievable under SRP increases, whereas that achievable under SMP decreases. That is, in networks with high node densities or transmission ranges, most of the antennas are exploited to increase throughput via spatial reuse instead of spatial multiplexing. It can then be concluded that the antennas are first exploited to increase spatial reuse by suppressing as much interference as possible, and then the remaining antennas, if any left, are exploited to increase data rates via spatial multiplexing.

The intuition behind this throughput behavior is as follows. Recall that when the transmission ranges and/or node densities are high, nodes' numbers of neighbors are likely to be high too. This increases path diversity by providing more paths for nodes to choose from when routing their traffic. In these situations, while SMP cannot exploit path diversity due to the fact that it can only use its DoFs to increase spatial multiplexing, SRP can take advantage of the increased number of paths to find better routes while effectively combating the interference, thus achieving more throughput. This explains why for a longer transmission range or a higher node density, the achievable throughput under SRP is greater than that under SMP.

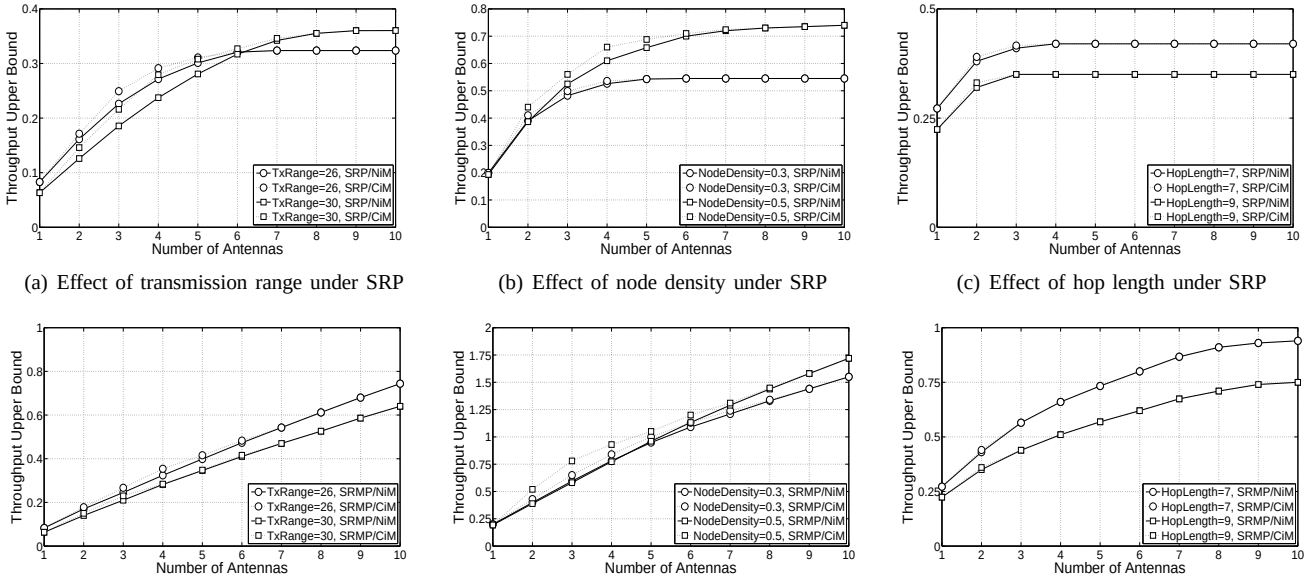

(a) Effect of transmission range under SRP (b) Effect of node density under SRP (c) Effect of hop length under SRP

(d) Effect of transmission range under SRMP (e) Effect of node density under SRMP (f) Effect of hop length under SRMP

Fig. 8. Non-cooperative vs. cooperative interference.

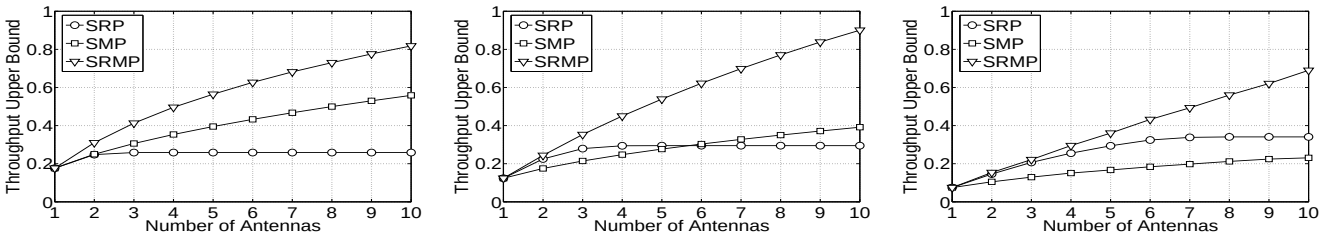

(a) $\texttt{TxRange} = 16$ (b) $\texttt{TxRange} = 22$ (c) $\texttt{TxRange} = 28$

Fig. 9. Effect of transmission ranges on the maximum achievable throughput under all MIMO protocols for $\texttt{N} = 50$ and $\texttt{Q} = 25$.

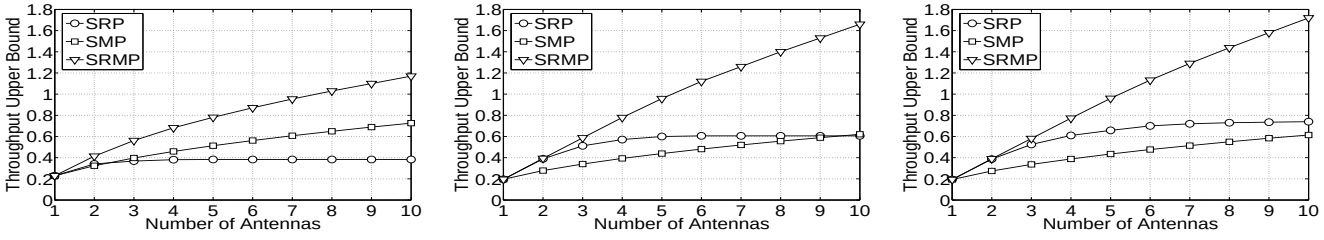

(a) $\texttt{NodeDensity} = 0.20\%$ (b) $\texttt{NodeDensity} = 0.35\%$ (c) $\texttt{NodeDensity} = 0.50\%$

Fig. 10. Effect of node densities on the maximum achievable throughput under all MIMO protocols for $\texttt{TxRange} = 30$ and $\texttt{Q} = 10$.

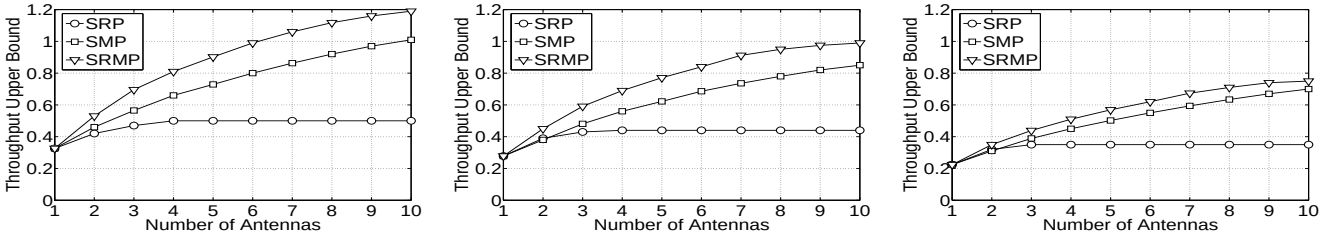

(a) $\texttt{HopLength} = 1$ (b) $\texttt{HopLength} = 5$ (c) $\texttt{HopLength} = 9$

Fig. 11. Effect of hop lengths on the maximum achievable throughput under all MIMO protocols for $\texttt{N} = 50$ and $\texttt{Q} = 25$.

Hop lengths, on the other hand, do not affect the performances of SRP and SMP vis-a-vis of each other. Fig. 11 shows that the throughput achievable under SMP is higher than that achievable under SRP and remains so despite the hop length. Note, however, that as the hop length increases, the throughput achievable under SMP degrades more significantly than that achievable under SRP. This is because greater hop lengths (i.e., longer routes) typically yield more interference, which limits the throughput obtainable under SMP.

VIII. Related Work

Due to its capabilities and promises, MIMO has been the focus of so many researchers for many years. As a result of this research effort, the limits and capabilities of MIMO in terms of throughput/capacity gain are now very well-understood [13], [4], [7], [24], [25], [6], [3], [26], [27], [28], but for the single, point-to-point, communication paradigm. The study of how much throughput/capacity MIMO can offer multi-hop wireless networks is, however, more recent and still in its infancy [29], [30], [31]. In [29], the authors introduced a new communication scheme for wireless ad hoc networks, where each MIMO-equipped node uses exactly one antenna when it transmits and uses all the antennas when it receives, and derived an upper bound on the average capacity that a single cell can achieve. In this new paradigm, a receiver uses its antennas to receive and decode multiple data streams from multiple different senders simultaneously. Jaafer *et al.* [30] investigated the per-node capacity in wireless mesh MIMO networks by studying the effect of the number of antennas that a node uses to transmit. The study, however, considers and evaluates the maximal achievable throughput in a chain-like topology. The work in [31] used a similar, LP-based method to also study throughput in multi-hop MIMO networks. It does not, however, account for cross-layer couplings effects, nor does it show how the total throughput behaves under different network scenarios and parameters. Unlike [31], our work (i) accounts for cross-layer effects through the modeling and use of effective degrees of freedom; (ii) models and studies two different interference avoidance approaches; (iii) investigates and studies throughput behavior for three different MIMO protocols; and (iv) provides a thorough simulation-based study of end-to-end throughput behavior under the effect of several network parameters, such as node density, transmission range, and MIMO size.

There have also been numerous studies on throughput/capacity characterization of wireless networks when nodes are equipped with single antennas [15], [32], [33], [34], [35]. Gupta and Kumar [15] derived the asymptotic capacity of multi-hop wireless networks of static nodes, each equipped with a single omnidirectional antenna. The work in [32] shows that per-user throughput can increase dramatically when nodes are mobile rather than fixed by exploiting a form of multiuser diversity via packet relaying. Several other studies have also focused on characterizing the capacity in multi-channel wireless networks [33], [34], [35]. The work in [15] has been extended in [33] to multi-channel wireless networks where nodes, each equipped with multiple interfaces, cannot have a dedicated interface per channel. Their results show that the capacity of such networks depends on the ratio of the number of channels to the number of interfaces. Alicherry *et al.* [34] developed a solution for routing in multi-channel, multi-interface wireless mesh networks that maximizes the overall throughput of the network subject to fairness and interference constraints. Along the same line, the work in [35] provides necessary conditions for the feasibility of rate vectors in multi-channel wireless networks with multiple interfaces, and use them to find upper bounds on throughput via a fast primal-dual LP algorithm. In this work, we adapt the LP constraint relaxation technique from [35] to characterize and analyze the maximum throughput that multi-hop wireless networks can achieve when equipped with MIMO links.

IX. Summary & Future Work

This paper models the interference and radio constraints of multi-hop wireless MIMO networks under the three proposed MIMO protocols, SRP, SMP, and SRMP, and the two proposed interference avoidance models, NiM and CiM. An optimal design problem is formulated as a standard LP whose objective is to maximize the network throughput subject to these constraints. By solving multiple instances of the formulated problem, we were able to characterize and analyze the maximum achievable throughput in multi-hop wireless MIMO networks. We study the effects of several network parameters on the achievable throughput, and illustrate how these results can be used by designers to determine the optimal parameters of multi-hop wireless MIMO networks.

This work assumes that a transmitter/receiver must have enough degrees of freedom to null/suppress its interference entirely before it can successfully send/receive its signal. In practice, however, a node may still be able to decode its signal even in the presence of some interference if the incurred interference does not make the signal to interference ratio drop below a certain threshold. This relaxation may improve the network throughput even further. As a future work, one can evaluate the total achievable network throughput (we are currently investigating this problem) under such a relaxation.

References

[1] *FCC, Spectrum Policy Task Force (SPTF), Report of the Spectrum Efficiency WG, November*, 2002.

[2] *XG Working Group. XG Vision RFC v2.0*.

[3] R. Narasimhan, "Spatial multiplexing with transmit antenna and constellation selection for correlated MIMO fading channels," *IEEE Transactions on Signal Processing*, vol. 51, no. 11, Nov. 2003.

[4] R. S. Blum, "MIMO capacity with interference," *IEEE Journal on Sel. Areas in Comm.*, vol. 21, no. 5, pp. 793–801, June 2003.

[5] Q. H. Spencer, A. Lee Swindlehust, and M. Haardt, "Zero-forcing methods for downlink spatial multiplexing in multiuser MIMO channels," *IEEE Tran. on Signal Processing*, vol. 52, no. 2, Feb. 2004.

[6] S. K. Jayaweera and H. Vincent Poor, "Capacity of multiple antenna systems with both receiver and transmitter channel state information," *IEEE Tran. on Infor. Theory*, vol. 49, no. 10, Oct. 2003.

[7] T. Marzetta and B. M. Hochwald, "Capacity of mobile multiple antenna communication link in rayleigh flat fading," *IEEE Tran. on Infor. Theory*, vol. 45, no. 1, pp. 139–157, January 1999.

[8] J. C. Mundarath, P. Ramanathan, and B. D. Van Veen, "A cross-layer scheme for adaptive antenna array based wireless ad hoc networks in multipath environment," *Wireless Networks*, Oct. 2007.

[9] K. Sundaresan, R. Sivakumar, M. A. Ingram, and T-Y Chang, "A fair medium access control protocol for ad-hoc networks with MIMO links," in *INFOCOM*, 2004.

[10] A. Nasipuri, S. Ye, J. You, and R. E. Hiromoto, "A MAC protocol for mobile ad hoc networks using directional antennas," in *WCNC*, Sep. 2000.

[11] L. Bao and J. J. Garcia-Luna-Aceves, "Transmission scheduling in ad hoc networks with directional antennas," in *MOBICOM*, 2002.

[12] R. R. Choudhury, X. Yang, R. Ramanathan, and N. H. Vaidya, "Using directional antennas for medium access control in ad hoc networks," in *MOBICOM*, 2002.

[13] T. Korakis, G. Jakllari, and L. Tassiulas, "A MAC protocol for full exploitation of directional antennas in ad-hoc wireless networks," in *MOBIHOC*, 2003.

[14] S. Yi, Y Pei, and S. Kalyanaraman, "On the capacity improvement of ad hoc wireless networks using directional antennas," in *MOBIHOC*, 2003.

[15] P. Gupta and P. R. Kumar, "The capacity of wireless networks," *IEEE Trans. on Infor. Theory*, vol. 2, no. 46, pp. 388–404, March 2000.

[16] A. U. Bhobe and P. L. Perini, "An overview of smart antenna technology for wireless communications," in *IEEE Aerospace Conference.*, March 2001, vol. 2, pp. 875–883.

[17] Y. S. Choi, P. J. Voltz, and F. A. Cassara, "On channel estimation and dectection for multicarrier signals in fast and selective rayleigh fading channels," *IEEE Transactions on Communications*, August 2001.

[18] B. Muquet and M. de Courville, "Blind and semi-blind channel identification methods using second order statistics for OFDM," in *Proceedings of IEEE Int'l Conference Acoustics, Speech, and Signal Processing*, March 1999.

[19] M. C. Necker and G. L. Stuber, "Totally blind channel estimation for OFDM on fast varying mobile radio channels," *IEEE Transactions on Wireless Communications*, September 2004.

[20] D. Gesbert, H. Bolcskei, D. Gore, and A. Paulraj, "Outdoor MIMO wireless channels: Models and performance prediction," *IEEE Transactions on Communications*, December 2002.

[21] J. C. Mundarath, P. Ramanathan, and B. D. Van Veen, "NULLHOC: A MAC protocol for adpative antenna array based wireless ad hoc netowrks in multipath environments," in *Proc. of IEEE GLOBECOM*, 2004.

[22] B. Hamdaoui and P. Ramanathan, "A cross-layer admission control framework for wireless ad-hoc networks using multiple antennas," *IEEE Transactions on Wireless Communications*, Nov. 2007.

[23] B. Hamdaoui and P. Ramanathan, "Cross-layer optimized conditions for QoS support in multi-hop wireless networks with MIMO links," *IEEE Journal on Selected Areas in Communications*, May 2007.

[24] G. J. Foschini and M. J. Gans, "On limits of wireless communications in a fading environment when using multiple antennas," *Wireless Personal Communications*, vol. 40, no. 6, 1998.

[25] M. Dohler and H. Aghvami, "On the approximation of MIMO capacity," *IEEE Transactions on Wireless Communications*, vol. 4, no. 1, January 2005.

[26] G. J. Foschini, D. Chizhik, M. J. Gans, C. Papadias, and R. A. Valenzuela, "Analysis and performance of some basic space-time architectures," *IEEE Journal on Selected Areas in Communications*, vol. 21, no. 3, April 2003.

[27] V. Tarokh, N. Seshadri, and A. R. Calderbank, "Space-time codes for high data rate wireless communication: Performance criterion and code construction," *IEEE Transactions on Information Theory*, vol. 40, no. 2, March 1998.

[28] Z. Chen, J. Yuan, and B. Vucetic, "Analysis of transmit antenna selection/maximal-ratio combining in rayleigh fading channels," *IEEE Transactions on Vehicular Technology*, vol. 54, no. 4, July 2005.

[29] X. Yu, R. M. Moraes, H. Sadjadpour, and J. J. Garcia-Luna-Aceves, "Capaicty of MIMO mobile wireless ad hoc networks," in *Proceedings of IEEE Int'l Conf. on Wireless Networks, Communications and Mobile Computing*, 2005.

[30] W. Jaafar, W. Ajib, and S. Tabbane, "The capaicty of MIMO-based wireless mesh networks," in *Proceedings of IEEE ICON*, 2007.

[31] R. Bhatia and L. Li, "Throughput optimization of wireless mesh networks with mimo links," in *Proceedings of IEEE INFOCOM*, 2007.

[32] M. Grossglauser and D. N. C. Tse, "Mobility increases the capacity of ad hoc wireless networks," *IEEE/ACM Transactions on Networking*, vol. 10, no. 4, pp. 477–486, August 2002.

[33] P. Kyasanur and N. H. Vaidya, "Capacity of multi-channel wireless networks: imapct of number of channels and interfaces," in *MOBICOM*, 2005.

[34] M. Alicherry, R. Bhatia, and L. Li, "Joint channel assignment and routing for throughput optimization in multi-channel wireless mesh networks," in *MOBICOM*, 2005.

[35] M. Kodialam and T. Nandagopal, "Characterizing the capacity region in multi-hop multi-channel wireless mesh networks," in *MOBICOM*, 2005.

PLACE PHOTO HERE

Bechir Hamdaoui received the Diploma of Graduate Engineer from the National School of Engineers at Tunis (BAC+6+DEA, ENIT), Tunisia, in 1997. He also received M.S. degrees in both Electrical & Computer Engineering (2002) and Computer Sciences (2004), and Ph.D. degree in Computer Engineering (2005) all from the University of Wisconsin at Madison.

From 1998 to 1999, he worked as a quality control and planning engineer on a power generation plant project under the supervision of PIRECO/FIAT Avio. He was an intern at Telcordia Technologies during the summer of 2004. In September of 2005, he joined the Real-Time Computing Research Lab at the University of Michigan at Ann Arbor as a postdoctoral researcher. Since September of 2007, he has been with the School of Electrical Engineering and Computer Science at Oregon State University as an assistant professor. His research spans various disciplines in the areas of computer networks and wireless communications systems. His current research focus is on protocol design and development, cross-layer performance modeling and analysis, QoS and admission control, and opportunistic resource usage and sharing. He is presently an Associate Editor for Hindawi Journal of Computer Systems, Networks, and Communications. He served as the program co-chairman of the IEEE PerCom Pervasive Wireless Networking Workshop (2009), and the program chair of the IWCMC WiMAX/WiBro Services and QoS Management Symposium (2009). He is a member of IEEE, IEEE Computer Society, and IEEE Communications Society.

PLACE PHOTO HERE

Kang G. Shin is the Kevin and Nancy O'Connor Professor of Computer Science and Founding Director of the Real-Time Computing Laboratory in the Department of Electrical Engineering and Computer Science, The University of Michigan, Ann Arbor, Michigan.

His current research focuses on QoS-sensitive networking and computing as well as on embedded real-time OS, middleware and applications, all with emphasis on timeliness and dependability. He has supervised the completion of 60 PhD theses, and authored/coauthored about 700 technical papers (more than 240 of which are in archival journals) and numerous book chapters in the areas of distributed real-time computing and control, computer networking, fault-tolerant computing, and intelligent manufacturing. He has co-authored (jointly with C. M. Krishna) a textbook "Real-Time Systems," McGraw Hill, 1997.

He has received a number of best paper awards, including the IEEE Communications Society William R. Bennett Prize Paper Award in 2003, the Best Paper Award from the IWQoS'03 in 2003, and an Outstanding IEEE Transactions of Automatic Control Paper Award in 1987. He has also received several institutional awards, including the Research Excellence Award in 1989, Outstanding Achievement Award in 1999, Distinguished Faculty Achievement Award in 2001, and Stephen Attwood Award in 2004 from The University of Michigan; a Distinguished Alumni Award of the College of Engineering, Seoul National University in 2002; 2003 IEEE RTC Technical Achievement Award; and 2006 Ho-Am Prize in Engineering.

He received the B.S. degree in Electronics Engineering from Seoul National University, Seoul, Korea in 1970, and both the M.S. and Ph.D degrees in Electrical Engineering from Cornell University, Ithaca, New York in 1976 and 1978, respectively.